UNITED STATES NAVY
AND
UNITED STATES AIR FORCE

PROJECT SQUID

TECHNICAL MEMORANDUM NO. CAL-36

ON THE PERFORMANCE ANALYSIS
OF THE
DUCTED PULSEJET

by

George Rudinger

OCTOBER 1951

CORNELL AERONAUTICAL LABORATORY, INC.
BUFFALO, NEW YORK

TECHNICAL MEMORANDUM NO. CAL-36

PROJECT SQUID

A COOPERATIVE PROGRAM
OF FUNDAMENTAL RESEARCH IN JET PROPULSION
FOR THE
OFFICE OF NAVAL RESEARCH, DEPARTMENT OF THE NAVY
AND THE
OFFICE OF AIR RESEARCH, DEPARTMENT OF THE AIR FORCE
Contract N6-ori-119, Task Order 1
NR 220-041
DD-420-A-36

ON THE PERFORMANCE ANALYSIS OF THE DUCTED PULSEJET

By

George Rudinger

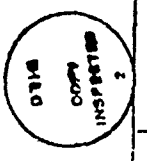

October 1951

CORNELL AERONAUTICAL LABORATORY, INC.
Buffalo, New York

ABSTRACT

Ducting of a pulsejet is a means to keep the engine operating at flight Mach numbers at which unducted conventional engines would not operate. It also allows the primary engine to take advantage of the possible ram precompression which is not utilized in the case of conventional pulsejets.

Since no methods are available to analyze in detail the periodic flow phenomena that occur in engines of this type, some approximate method of performance calculation is required. Depending on the shroud configuration, mixing of the pulsejet exhaust with the remaining shroud flow may or may not take place. In the latter case, methods of analysis developed for single-flow engines may be applied while in the former, only the equivalent steady flow approximation appears to be feasible at the present time.

Estimates are derived for the magnitude of the flow pulsations in the shroud and on the basis of this, a discussion of the equivalent steady flow approximation is presented.

Unfortunately, it is found that only a rough estimate of the potential engine performance can be made. However, from the performance computed for various conditions, it is possible to draw certain conclusions about the merits of various configurations.

TABLE OF CONTENTS

I. INTRODUCTION

Successful operation of conventional pulsejets has so far been limited to comparatively low flight velocities. As the velocity is increased, the increasing ram pressure at the inlet valves requires a higher combustion pressure to keep the valves closed over a sufficiently long fraction of each cycle; on the other hand, back flow through the tail exit and precompression are reduced and it becomes more and more difficult for the combustion process even to maintain the pressures observed during static operation of the engine. Eventually, the valves remain open for too great a fraction of each cycle and in the vicinity of a flight Mach number of 0.6 the engine will cease to resonate[1].

Attempts are being made to extend the useful operating range of pulsejets to higher flight Mach numbers. One such approach is to place the pulsejet inside a shroud which is designed to keep the flow around the engine at a low Mach number at all times. In a power plant of this type, known as a ducted, or shrouded, pulsejet, the detrimental pressure difference between ram pressure at the inlet valves and static pressure at the tail pipe exit is practically eliminated and with a suitable shroud design it should therefore be possible to keep the engine operating at any flight Mach number. Furthermore, this scheme allows the primary engine to make full use of the possible ram precompression which is not utilized in conventional pulsejets.

The schematic construction of a ducted pulsejet is shown in Fig. 1. Air enters the shroud through the inlet diffuser where it is slowed down to a low Mach number. Part of this flow is required for the operation of the pulsejet and after being exhausted from the latter, mixes with the remaining shroud flow. Finally, the gases are returned to the atmosphere through the exit nozzle.

Several variations of this basic configuration may be considered. The pressure at the pulsejet valves is primarily determined by the flight velocity irrespective of whether or not the shroud is present. An alternative to the completely ducted engine of Fig. 1 is therefore a type where only the tail pipe of the pulsejet is submerged in a shroud; this configuration will be referred to as tail ducted engine.

Mixing of the pulsejet exhaust with the surrounding shroud flow is not always beneficial; therefore, the two extreme cases will be considered: (a) engines with a shroud that is long enough to insure complete mixing, and (b) engines where the shroud is so short that mixing is eliminated.

The intermittent action of the primary engine produces a periodically pulsating flow that cannot be analyzed in detail at the present time and some approximate method to estimate the potential performance of the ducted pulsejet is therefore needed. Engines in which no mixing takes place can be treated essentially in the same manner as single-flow engines and the method recently given by Foa[2] may therefore be applied. In the case of configurations that involve mixing, it seems that the only method of analysis that is available at the present time is the "equivalent steady flow" approximation. This method is based on the consideration that if the flow pulsations are sufficiently small, the mean values of the flow parameters may be used to characterize a steady flow that would be equivalent in its effects to the actual pulsating flow in spite of the nonlinearity of the gasdynamics relations. Whether or not such an approach would lead to reliable results in the case of the ducted pulsejet depends therefore on the magnitude of the flow pulsations in the shroud.

A previous investigation[3] was based on this concept of an equivalent steady flow. In this preliminary study this approach was, a priori, assumed to be valid (see, however, footnote on page 20). In the following, an estimate for the magnitude of the flow pulsations in the shroud is derived and on the basis of this, a more detailed discussion of the equivalent steady flow approximation is presented. Unfortunately, it is found that only a rough estimate of the potential performance of the ducted pulsejet can be obtained. It is possible, however, to reach certain conclusions about the effects of flight speed and the merits of the various shroud configurations referred to above.

At the time of completion of this manuscript, a paper by Sänger[4] came to the author's attention which is a general study of ducted steady-flow power plants. A short portion of the paper is also devoted to the ducted pulsejet, however, without discussion of the validity of this approach. Although no direct comparison of results is possible, there is substantial agreement on certain conclusions reached.

II LIST OF SYMBOLS

The analysis of one-dimensional-flow problems is greatly facilitated by the use of certain functions of the Mach number and tables of these functions[5]. These functions are defined below where also a number of identities and definitions are given that will be used in the course of the calculations.

The following symbols and units will be used:

a	ft/sec	speed of sound
A	ft^2	cross sectional area
c_p	Btu/lb, ^oR	specific heat at constant pressure
D	-	$= M\left(1+\frac{\gamma-1}{2}M^2\right)^{-\frac{\gamma+1}{2(\gamma-1)}}$
F	lb	stream force = $pA + \dot{m}u$
g	ft/sec^2	acceleration due to gravity
G	-	$= (1+\gamma M^2)\left(1+\frac{\gamma-1}{2}M^2\right)^{-\frac{\gamma}{\gamma-1}}$
h	Btu/lb	heating value of fuel
I_a	sec.	air specific impulse = $\frac{T}{g\dot{m}} = \frac{u_e - u_o}{g}$
I_f	sec.	fuel specific impulse = αI_a
k	-	uncertainty factor (defined in Section IV.A)
m	slug	mass
$\dot{m}$	slug/sec	air mass flow = $\rho A u \cdot \sqrt{\frac{\gamma}{R}}\ \frac{pAM}{\sqrt{\gamma}}$ · $= \sqrt{\frac{\gamma}{R}}\ \frac{PAD}{\sqrt{\theta}}$

M	–	Mach number = $\frac{u}{a}$
$\mathcal{M}$	–	shock Mach number (Mach number of the supersonic flow ahead of a shock, relative to the shock wave)
$\mathcal{M}'$	–	Mach number of the subsonic flow behind a shock relative to the shock wave
$\mathcal{A}$	–	ratio of downstream to upstream stagnation pressures across a shock wave[5]
p	lb/ft^2	static pressure
P	lb/ft^2	stagnation pressure
q	Btu/lb	heat added per pound of air
		mass flow ratio = $\frac{\langle \dot{m}_a \rangle_{av}}{\langle \dot{m}_j \rangle_{av}}$
R	ft.lb/slug,^oR	gas constant
s	Btu/lb.^oR	specific entropy
t	sec.	time
T	lb.	thrust = $\dot{m}(u_e - u_o)$
u	ft/sec.	flow velocity relative to power plant
U	ft/sec.	shock velocity relative to power plant
α	–	air/fuel ratio
γ	–	ratio of specific heats
η_c	–	combustion efficiency
θ	^oR	static temperature
Θ	^oR	stagnation temperature
μ	slug	mass per cycle
ρ	$slug/ft^3$	gas density
σ	–	= P_1 / P_o
τ	sec.	period of pulsejet oscillations

Subscripts

Subscripts 1, 2, 3.... etc. refer to flow conditions that are identified in Figs. 2 and 4, respectively.

i	initial shock wave in the tail pipe of the pulsejet that is produced by an explosion in the combustion chamber	
u	upstream moving shock waves	
d	downstream moving shock waves	
o	free stream conditions relative to power plant	
t	throat of the inlet diffuser	equivalent steady flow conditions
a	exit of shroud inlet diffuser	
b	inlet of shroud exit nozzle	
e	shroud exit	
j	pulsejet exit	instantaneous values
s	annular space of the shroud at the location of the pulsejet exhaust	
P	characteristics of the primary pulsejet	
n	normal sea level conditions	

$\overline{(\ )}$ mass average of a parameter over one period of the pulsejet,

e.g., $$\bar{s} = \frac{1}{\mu}\int_0^{\mu} s \, dm$$

$\langle\ \rangle_{av}$ time average of a parameter over one period of the pulsejet,

e.g., $$\langle p \rangle_{av} = \frac{1}{\tau}\int_0^{\tau} p \, dt$$

III THE MAGNITUDE OF THE FLOW PULSATIONS IN THE SHROUD OF A DUCTED PULSEJET

Pressure waves in the shroud of a ducted pulsejet originate both at the inlet valves and at the tail exit of the primary engine. This Section represents an attempt to estimate the magnitude of the variations of the state and flow parameters in the shroud.

The pressure waves are reflected from various points in the shroud and superpose new waves created in the following cycles, until eventually, a periodic flow field is established. Nonsteady flows in ducts are usually studied by means of the method of characteristics[6]. This method, however, requires the knowledge of the initial conditions in the duct which are not known in the case of periodic flow phenomena. It is therefore necessary to assume an initial steady flow in which the pressure waves are generated. In the cases considered here, the extreme variation of the state and flow parameters can then be estimated from the initial waves of a characteristics diagram.

The flow in the inlet diffuser divides into two branches that merge again downstream of the pulsejet exhaust. These "branched flows" were studied using the relations that apply to one-dimensional flows. The solutions become therefore valid only at some distance from the branching points. The analysis was carried out separately for each branching point.

A. Pressure waves originating at the pulsejet inlet

The lowest pressure and highest flow velocity at the pulsejet valves occurs while the valves are open and inflow takes place. When the air-fuel mixture in the combustion chamber explodes, the valves close rapidly which causes the pressure ahead of the valves to rise to its maximum and the flow velocity to drop to its minimum value. The rapid pressure rise produces pressure waves, treated approximately as shock waves, that are travelling

upstream toward the shroud inlet and downstream around the pulsejet, respectively. These waves and their paths in a time–position plane are indicated in Fig. 2. It is assumed that the open valves do not block the flow at all so that the velocity with which the flow enters the pulsejet is equal to that of the flow around the pulsejet.

Let all parameters during the inflow period be denoted by subscript 1. After passage of the waves, the modified parameters upstream of the inlet valves and of the flow around the pulsejet will be characterized by subscripts 2 and 3, respectively. The regions in which these subscripts apply are also indicated in Fig. 2.

When the valves close, the area available to the flow contracts from its initial value A_{max} to a value A_3. The strength of the two shock waves produced depends on the initial flow conditions and on the area ratio A_3 / A_{max}.

Let all velocities u be measured relative to the duct and positive in the downstream direction and let the speed of sound be denoted by a.

From the velocity U_u of the upstream moving shock wave, the shock Mach number (i.e., the Mach number of the supersonic flow relative to the shock) follows as

$$\mathcal{M}_u = \frac{u_1 - U_u}{a_1} = M_1 - \frac{U_u}{a_1} \quad . \tag{1}$$

The Mach number of the subsonic flow behind the shock and relative to the shock becomes

$$\mathcal{M}_u' = \frac{u_2 - U_u}{a_2} = M_2 - \frac{U_u}{a_1}\frac{a_1}{a_2} \quad . \tag{2}$$

Eqs. (1) and (2) combine to

$$M_2 = (M_1 - \mathcal{M}_u)\,\frac{a_1}{a_2} + \mathcal{M}_u' \quad . \tag{3}$$

Denoting the Mach number of the downstream moving shock by $\mathcal{M}_d$, one obtains in the same way

$$M_3 = (M_1 + \mathcal{M}_d)\,\frac{a_1}{a_3} - \mathcal{M}_d' \quad . \tag{4}$$

Since the modified flow behind the two shock waves is again steady, the mass flow must be the same in regions 2 and 3 with the same value of the stagnation temperature θ . If the flow around the pulsejet is considered to be isentropic, the stagnation pressure P must also be the same in the two regions and, therefore, the relation

$$A_{max}\, D_2 = A_3\, D_3 \tag{5}$$

holds (see List of Symbols for mass flow).

For any value of $\mathcal{M}_u$, the parameters $\mathcal{M}_u$, a_2/a_1 and p_2/p_1 , and for any $\mathcal{M}_d$, the parameters $\mathcal{M}_d'$, a_3/a_1 and p_3/p_1 can be obtained from the Rankine-Hugoniot shock relations or from a table of these relations, e.g., reference 5. Auxiliary graphs can then be prepared on the basis of Eqs. (3) and (4) in which the parameters D_2 and $P_2/p_1 = (P_2/p_2)(p_2/p_1)$ are plotted versus $\mathcal{M}_u$ and, similarly, D_3 and P_3/p_1 versus $\mathcal{M}_d$ for selected values of M_1 . Since $P_2 = P_3$, one may obtain from these graphs pairs of values D_2 and D_3 for any value of $\mathcal{M}_u$. The area ratio A_3/A_{max} that corresponds to the assumed value of $\mathcal{M}_u$ follows then from Eq. (5).

The results of these calculations are shown in Fig. 3 where the strength of the upstream travelling shock wave is plotted versus the area ratio A_3/A_{max}, for values of the initial Mach number M_1 ranging from 0.2 to 0.5. The shock strength is expressed both by the pressure ratio across the shock p_2/p_1 and by the shock Mach number $\mathcal{M}_u$. For the two extreme values of M_1, the corresponding curves for the downstream travelling shock wave are also entered as dashed lines.

In any actual engine, the fraction of the flow in the shroud that is not interrupted by the closure of the valves, (A_3/A_{max}), will generally be greater than about 0.4, and the maximum Mach number at the exit of the inlet diffuser will probably not exceed 0.35. Under these conditions, the pressure ratio p_2/p_1 would be less than 1.30. Since the mean value of the pressure would be somewhere near the middle of its range of variation, the amplitude of the pressure oscillations could thus be estimated to be at most 15% of the mean pressure and in many cases it could be expected to be considerably smaller.

B. Pressure waves originating at the pulsejet exhaust

The area of the tail pipe exit of the pulsejet is denoted by A_j and the maximum shroud area again by A_{max}. As before, it is necessary to assume a steady initial state. Let subscripts 1, 2, and 3 refer to the conditions in the shroud downstream of the tail pipe exit, upstream of the tail pipe exit, and inside the tail pipe, respectively. Inflow into the tail pipe of the pulsejet has practically ceased just before the exhaust period starts and therefore the assumption is made that in the tail pipe the flow velocity is zero and the temperature is equal to the stagnation temperature in the shroud. The duct area that is available to the shroud flow suddenly widens at

the location of the tail pipe exit so that the flow from region 2 to region 1 is not isentropic. The initial pressure wave that is produced by the explosion in the combustion chamber of the pulsejet is approximated by a shock wave of shock Mach number M_i . The conditions in the tail pipe following the shock wave are characterized by subscript 4 (see Fig. 4a).

The shock wave is reflected from the tail pipe exit as an expansion wave and the pressure rise in the shroud is propagated upstream and downstream by two shock waves of strength M_u and M_d , respectively. The subscripts used in the various regions after reflection of the primary shock wave are indicated in Fig. 4b. The pulsejet exhaust mixes with the modified shroud flow and subscript 7 refers to the completely mixed conditions. Downstream of the mixing region, and separated from it by an interface, is the flow that has been modified by the downstream moving shock wave (region 8). The path of the various waves in a time-position plane is shown in Fig. 4c which is drawn in two parts to show the relation between the conditions downstream of the pulsejet exit, and the flows in the tail pipe and in the shroud, respectively.

The problem is to find the strength M_u and M_d of the created shock waves for a given configuration A_j / A_{max} , initial flow conditions, and strength M_i of the initial shock wave. The calculations are essentially similar to those used in the previous Section but they are considerably more lengthy since mixing of the exhaust jet and the shroud flow must also be considered. Solutions can only be obtained by a trial and error procedure. Guessing the value of p_6 / p_1 and setting $p_6 = p_5$ (unless the pulsejet exhaust becomes sonic or supersonic in which case the exhaust Mach number and not the pressure determines the wave reflection in the tail pipe) enables one to compute the exhaust flow and the modified shroud flow upstream of the

tail pipe exit. Conditions 7 are then determined from standard mixing relations for constant area mixing. Across the interface that separates regions 7 and 8, pressure and velocity do not change and either of these parameters leads to the strength M_d of the downstream travelling shock wave. Unless the two values of M_d thus obtained coincide, the original guess must be modified until agreement is reached.

The results of these calculations are shown in Figs. 5 and 6. The computations were limited to two geometrical configurations, namely $A_j / A_{max} = 0.6$ and 0.4, respectively, which enclose the range most likely to be encountered in actual engines. The initial flow conditions were prescribed by $M_1 = 0.1$, 0.2 and 0.3, respectively, and the Mach number of the initial shock wave was varied between 1.0 and 1.6 corresponding to pressure ratios p_4 / p_3 between 1 and approximately 2.8.

Fig. 5 shows that the upstream moving shock waves are comparatively weak. Their strength does not increase continually as the strength of the initial shock increases but reaches a maximum value and then decreases again. Qualitatively, this may be explained as follows: With increasing strength of the initial shock wave, the pressure at the tail pipe exit would tend to rise thus decelerating the flow around the tail pipe. At the same time the outflow from the tail pipe acts as an ejector jet in the surrounding flow, accelerating it, and thus tending to decrease the strength of the upstream moving shock wave. The maximum of the curves in Fig. 5 results from the interaction of these two opposing effects. Actual pressure measurements taken at a point close to the tail pipe exit of small pulsejet models indicated that the ratio between the maximum and the minimum pressure there is somewhat in excess of two*.

*These experiments were carried out with a small pulsejet model (tail pipe diameter of 3 in.). A condenser type pressure gauge[7] was mounted one inch from the tail pipe exit, and the pressure fluctuations were recorded by means of a cathode ray oscilloscope and a strip camera.

This would correspond to points close to the maxima of the curves in Fig. 5. For the required low values of M_2 , the corresponding values of M_6 would then be extremely low. One is therefore led to the conclusion that in a ducted pulsejet, the shroud flow around the tail pipe is practically brought to rest periodically by the exhaust from the primary pulsejet. Evidence supporting this conclusion was obtained by experiments that are described in the Appendix.

In Fig. 6, the strength of the downstream moving shock wave is plotted versus the strength of the primary shock wave for the two analyzed configurations and various initial flow conditions. As one would anticipate, the pressure fluctuations downstream of the mixing region are still quite large but they are considerably smaller than those at the location of the pulsejet exhaust. Their strength increases continually with that of the primary wave.

IV ANALYSIS OF THE DUCTED PULSEJET

The schematic design of a ducted pulsejet was shown in Fig. 1 and possible variations of the shroud configuration have already been pointed out in Section I. Depending on whether or not mixing of the pulsejet exhaust with the surrounding duct flow takes place, different methods of attack are required which are based on certain assumptions and approximations that will be discussed in the course of the analysis. Those assumptions, however, that apply in either case are collected here:

The air flowing through the engine is treated as an ideal gas with constant values of the specific heats. The effects of the mass of the injected fuel are neglected. All flows are treated as one-dimensional.

Since the primary purpose of this study is an attempt to develop a method of performance analysis, losses do not occupy the important position which they normally assume in engineering applications. For this reason, losses due to wall friction are not taken into account since they would introduce complications that are not considered justified at this stage.

Allowance for incomplete combustion is made; this merely requires a correction factor (combustion efficiency) to be applied to the heat released by the fuel.

Shock losses at supersonic flight speeds reduce the stagnation pressure that is available at the pulsejet inlet from the free stream value P_o to $P_a = \sigma P_o$. The value of σ depends on the configuration under investigation. If the shroud completely surrounds the pulsejet, as illustrated in Fig. 1, it was shown in the previous Section that the strength of the upstream travelling pressure waves is quite small. It seems therefore reasonable to assume that the shock losses in this case are essentially the same as in a steady flow with the shock located at the optimum position in the diffuser. All calculations are based on a Kantrowitz-Donaldson diffuser[8] designed for the flight Mach number considered. The throat Mach number for this diffuser is given by the relation[5] $D_t = 0.5787\ \mathcal{M}_o$ where $\mathcal{M}$ denotes the Mach number function that is equal to the ratio of downstream and upstream stagnation pressures of a shock wave. Thus, diffuser shock losses are allowed for by setting $\sigma = \mathcal{M}_t$.

In a tail ducted engine, the pressure waves created by the closing of the valves cannot dissipate part of their strength in the flow around the pulsejet. Shock losses are therefore larger in this case than in the previous one and they are assumed to be equal to those corresponding to a

normal shock at flight Mach number, as was done in previous analyses[2),(3)]. In this case, one has simply $\sigma = \mathcal{N}_0$.

The atmospheric temperature enters in the calculations. A value of 460°R (corresponding to an altitude of about 16,000 feet) is used but the effect of deviations from a reasonable average temperature is quite negligible[(2),(3)].

A. Engines with complete mixing of the pulsejet exhaust with the shroud flow

The problem of dealing with periodic flows in which the amplitude of the pulsations is not negligible, is further complicated in this engine configuration because mixing of two nonsteady flows must also be considered. It seems that, at the present time, the "equivalent steady flow" approximation offers the only possible approach.

It was shown in the previous Section that the upstream travelling pressure waves in the shroud are quite weak and the use of steady-flow relations seems therefore justified for the flow in the diffuser exit - station a (Fig.1). The average values of the flow parameters at this station will be denoted by subscript a.

At station b which is located at that section of the shroud where mixing is completed the flow pulsations are still of considerable magnitude. If one imagines now an extremely long extension of the duct, the compression and expansion waves in the flow would gradually overtake and cancel each other and all temperature gradients would disappear due to heat conduction between gas layers of different temperatures. Thus, the flow would ultimately become steady although its entropy would then be higher than the mean entropy of the completely mixed but still pulsating flow. The use of the "equivalent steady flow" approximation for the exhaust of the ducted pulsejet should only be considered in those cases where it can be shown that the additional entropy rise,

due to the flow becoming steady, is small compared to the mean entropy rise that the air undergoes from the free stream condition to the completely mixed but nonsteady state at station b. Since this additional entropy rise can only be computed for specific cases, an arbitrary flow with pulsations of a reasonable magnitude must be assumed. The following cyclic variations of the flow parameters were chosen:

$$\frac{p}{p_0} = 1 + 0.2 \cos 2\pi \frac{m}{\mu}$$

$$\frac{v}{v_0} = 2.6 \left(1 + 0.5 \cos 2\pi \frac{m}{\mu}\right)$$

$$M = 0.25 \left(1 + 0.4 \cos 2\pi \frac{m}{\mu}\right) .$$

Since the mean entropy is determined by the mass average and not by the time average, the above parameters are given as periodic functions of the mass m that has passed the station since the beginning of the cycle. The mass of air for one complete cycle is denoted by μ.

If the entropy level of the free stream is taken as zero, the entropy of any mass element is given by

$$\frac{s}{c_p} = \ln \frac{v}{v_0} - \frac{\gamma - 1}{\gamma} \ln \frac{p}{p_0} \qquad (6)$$

and the mean value of the entropy is then given by

$$\bar{s} = \frac{1}{\mu} \int_0^{\mu} s \, dm \quad . \qquad (7)$$

If the values for the state parameters are substituted here, the integral may be evaluated numerically. For the assumed flow conditions the result is $\bar{s}/c_p = 0.781$.

Subscript b will be used to denote the parameters of the equivalent steady flow which must be determined from the mean values of mass flow, energy flux and stream force since these three quantities must be the same for the steady and pulsating flows if they are to be considered equivalent.

The mass flow $\dot{m}_b$ is given by

$$\dot{m}_b = \frac{\mu}{\tau} \tag{8}$$

where τ, the period of the oscillations, follows from the relation

$$\tau = \int_0^{\mu} \frac{dm}{\dot{m}} = \frac{1}{p_* A_{max}} \sqrt{\frac{R v_0}{\gamma}} \int_0^{\mu} \frac{\sqrt{v/v_0}}{M(p/p_0)}\, dm \,. \tag{9}$$

The mean mass flow may therefore be obtained in the form

$$\sqrt{\frac{R v_0}{\gamma}}\, \frac{\dot{m}_b}{p_0 A_{max}} = \left(\frac{1}{\mu} \int_0^{\mu} \frac{\sqrt{v/v_0}}{M(p/p_0)}\, dm \right)^{-1} \tag{10}$$

The stagnation temperature of the equivalent steady flow is obtained from the condition that the energy flowing past a section during one cycle must be the same at all sections, or

$$\mu \theta_b = \int_0^{\mu} \theta\, dm .$$

It follows from this that

$$\frac{\theta_b}{v_0} = \frac{1}{\mu} \int_0^{\mu} \frac{v}{v_0} \left(1 + \frac{\gamma - 1}{2} M^2\right) dm. \tag{11}$$

The stream force F_b being derived from the momentum equation, must be obtained from the time average of the variable stream force F. In order to evaluate this time average, it must be transformed first into a mass average since the flow parameters were given as functions of mass rather than time. One can write for the mean stream force

$$F_b = \frac{1}{\tau}\int_0^{\tau} F\,dt = \frac{1}{\tau}\int_0^{\mu} \frac{F}{\dot{m}}\,dm = \frac{1}{\tau}\sqrt{\frac{R v_o}{\gamma}}\int_0^{\mu} \frac{1+\gamma M^2}{M}\sqrt{v/v_o}\;dm$$

where the last result is derived by expressing both F and $\dot{m}$ in terms of the given flow parameters. If one substitutes here for τ the value from Eq. (9), one obtains finally

$$\frac{F_b}{p_o A_{max}} = \frac{\int_0^{\mu} \frac{1+\gamma M^2}{M}\sqrt{v/v_o}\;dm}{\int_0^{\mu} \frac{\sqrt{v/v_o}}{M(p/p_o)}\,dm} \qquad (12)$$

The right hand sides of Eqs. (10), (11), and (12) can be evaluated by substituting the given flow parameters and integrating numerically. Because of the identities (see List of Symbols)

$$\sqrt{\frac{R v_o}{\gamma}}\,\frac{\dot{m}_b}{p_o A_{max}} = \frac{D_b (P_b/p_o)}{\sqrt{\theta_b/v_o}} \qquad (10a)$$

and

$$\frac{F_b}{p_o A_{max}} = \frac{G_b P_b}{p_o} \qquad (12a)$$

one can solve Eqs. (10), (10a), (11), (12), and (12a) first for $N_b = D_b/G_b$

and then by the use of tables of these Mach number functions[5] also for P_b / P_0. From this last quantity and Eq. (6), the entropy of the flow may be computed. The assumptions made above for the flow parameters lead to a value $s_b / c_p = 0.852$ which must be compared with the mean entropy of the pulsating flow of $\bar{s} / c_p = 0.781$.

In this case, which is believed to be fairly representative, the additional entropy rise due to the flow becoming steady in the hypothetical duct extension is therefore less than 10 percent of the mean entropy rise that the air undergoes from free stream conditions to the exhaust of the ducted pulsejet. The significance of this entropy error may be evaluated by means of a relation, derived by Foa[2], which expresses the entropy rise through a pulsejet as function of the air/fuel ratio, combustion efficiency, and mode of combustion (approximated by the exponent of a polytropic process). Using this relation, it can be verified that the combined effect of the unavoidable uncertainty of these parameters on the entropy rise in the engine is of the same order of magnitude as the entropy error introduced by the "equivalent steady flow" approximation.

On the basis of these entropy considerations alone, the use of steady flow relations for the engine exhaust would thus lead to results that are somewhat conservative. On the other hand, the thrust that is developed by a steady flow is always higher than that of a pulsating flow of same energy flux[2]. These two effects neither of which is large thus tend to cancel each other in their influence on the computed performance and it seems therefore justified to treat the exhaust of a ducted pulsejet in terms of steady-flow relations.

In the course of the following analysis, it will be possible to compute the mean values of mass flow and energy flux from the given data. However, the average stream force will only be obtained as an approximation. The reasons for this will be discussed below and the uncertainty of the stream force will be expressed by a factor applied to the computed average value.

It is now possible to build up a method of performance analysis for the ducted pulsejet. In addition to the general conditions listed at the beginning of this Section, it is necessary to make assumptions for the performance of the unducted pulsejet. Let T_p be the thrust of the pulsejet under the conditions prevailing inside the shroud, and T_{p_n} the thrust of the same engine at a flight velocity corresponding to the mean Mach number of the shroud flow but under standard sea level conditions (v_n, p_n). It may be assumed in reasonably good agreement with observations[1] that the thrust is proportional to the density of the surrounding air and because of the low Mach numbers of the shroud flow at station a, one may with sufficient accuracy take the stagnation instead of the static density at this station.

If A_j denotes the area of the pulsejet exhaust, the ratio T_{p_n}/A_j is one of the performance parameters of the primary pulsejet that must be assumed. The thrust inside the shroud* may therefore be expressed in form

$$T_p = T_{p_n} \frac{p_a}{\theta_a} \frac{v_n}{p_n}$$

*The thrust T_p is here defined as the change of momentum transport of the air that flows through the engine. In the previous analysis of the ducted pulsejet[3], the same value of T_p was incorrectly taken as the change of momentum transport including the flow around the engine. Since the contribution of the shroud flow, which will be determined in the following, may be a considerable drag, the results of the previous analysis must be considered as too optimistic.

or

$$\frac{T_p}{p_o A_{max}} = \frac{T_{pn}}{A_j} \frac{A_j}{A_{max}} \frac{\sigma}{\rho_n} \frac{v_n}{v_o} \left(1 + \frac{\gamma - 1}{2} M_o^2\right)^{\frac{1}{\gamma-1}} . \tag{13}$$

The fuel specific impulse I_{fp} and the air/fuel ratio α_p of the primary engine are assumed to remain unaltered when the engine is operating inside the shroud. Then the air specific impulse I_{ap} which is given by the ratio I_{fp}/α_p also remains constant and the mass flow through the pulsejet, $\langle \dot{m}_p \rangle_{av}$, may be calculated from the relation between these parameters and the thrust of the engine (see List of Symbols) as

$$\frac{\langle \dot{m}_j \rangle_{av}}{p_o A_{max}} = \frac{T_p / p_o A_{max}}{g I_{ap}} . \tag{14}$$

The design of the shroud is characterized not only by A_j / A_{max} but also by the inlet and exit configuration. These conditions determine how much of the mass flow that enters the shroud passes through the pulsejet, $\langle \dot{m}_j \rangle_{av}$, and how much flows around it, $\langle \dot{m}_s \rangle_{av}$. The ratio

$$r = \frac{\langle \dot{m}_s \rangle_{av}}{\langle \dot{m}_j \rangle_{av}} \tag{15}$$

thus represents a design parameter that may be given an arbitrarily selected value.

It is now possible to calculate all flow parameters at station a since $p_a = \sigma p_o$, $\theta_a = \theta_o$ and $\dot{m}_a / p_o A_{max} = (1+r)\langle \dot{m}_j \rangle_{av} / p_o A_{max}$.

The average stream force in the mixing region of the shroud is made up of two parts, namely, the stream force of the pulsejet exhaust $\langle F_j \rangle_{av}$ and the contribution of the duct flow around the pulsejet $\langle F_s \rangle_{av}$.

The following definitions apply

$$\langle F_j \rangle_{av} = A_j \langle p_j \rangle_{av} + \langle \dot{m}_j u_j \rangle_{av} = A_j \langle p_j \rangle_{av} + \frac{1}{\tau}\int_0^{\tau} \dot{m}_j u_j \, dt \qquad (16)$$

and

$$T_p = \frac{1}{\tau}\int_0^{\tau} \dot{m}_j u_j \, dt - \langle \dot{m}_j \rangle_{av} u_a \, . \qquad (17)$$

If viscous flow losses in the shroud are neglected, the flow from station a to station s is isentropic so that the mean Mach number may be computed from the relation

$$(A_{max} - A_j) \langle D_s \rangle_{av} = A_{max} \frac{r}{r+1} D_a \qquad (18)$$

from which $\langle D_s \rangle_{av}$ and a corresponding mean Mach number $M_{s\,mean}$ is obtained.

Since the shroud diameter is small compared to the wavelength of the pressure waves one may take the pressure at the location of the pulsejet exhaust as uniform across the entire section, or $p_j = p_s$ and thus set

$$\langle p_j \rangle_{av} = \frac{P_a}{\left(1 + \frac{\gamma - 1}{2} M_{s\,mean}^2\right)^{\frac{\gamma}{\gamma-1}}} \, . \qquad (19)$$

These relations are somewhat uncertain not only because losses in the rather narrow passage between shroud and pulsejet have been neglected but also because the unknown wave form of the cyclic variations of the parameters introduces an error in the computation of the mean Mach number. An allowance for this error will be made by an uncertainty factor applied to the computed mean stream force. In this manner, the seriousness of any error

introduced by this approximation may be evaluated by its effect on the final results.

When Eqs. (16), (17), and (19) are combined, one obtains

$$\frac{\langle F_j \rangle_{av}}{p_o A_{max}} = \frac{A_j}{A_{max}} \sigma \frac{P_o}{p_o} \left(1 + \frac{\gamma - 1}{2} M_{4\,mean}^2 \right)^{-\frac{\gamma}{\gamma - 1}} + \frac{\bar{T}_p}{p_o A_{max}} + \frac{\langle \dot{m}_j \rangle_{av} u_a}{p_o A_{max}} \quad . \quad (20)$$

The stream force contribution of the shroud flow is given by

$$\frac{\langle F_s \rangle_{av}}{p_o A_{max}} = \sigma \frac{P_o}{p_o} \left(1 - \frac{A_j}{A_{max}} \right) G_{4\,mean} \quad (21)$$

and therefore the stream force of the completely mixed flow is given by

$$\frac{F_b}{p_o A_{max}} = k \left(\frac{\langle F_j \rangle_{av}}{p_o A_{max}} + \frac{\langle F_s \rangle_{av}}{p_o A_{max}} \right) \quad (22)$$

where k is the uncertainty factor just referred to.

The stagnation temperature θ_b may be directly obtained from the free stream value θ_o and the amount of heat added to the entire flow per pound of air, q.

This parameter is given by $q = h \eta_c / \alpha$ where h and η_c denote the heating value of the fuel and the combustion efficiency, respectively. The over-all air/fuel ratio α is related to the air/fuel ratio of the pulse-jet by $\alpha = \alpha_p (1 + \mu)$, and θ_b is therefore given by

$$\theta_b = \theta_o + \frac{h \eta_c}{\alpha_p c_p (1 + \mu)} \quad . \quad (23)$$

Having computed the streamforce, mass flow and stagnation temperature at station b, one may obtain all other flow parameters in the same manner as was done in the example earlier in this Section. The flow at the exhaust nozzle, station e (Fig. 1), is easily obtained since the flow from station b

to station e may be treated as isentropic. The exhaust pressure is atmospheric and all flow parameters may therefore be obtained from the conditions

$$\theta_e = \theta_0$$
$$P_e = P_b$$
$$p_e = p_0 \ .$$

Once the exhaust conditions are known, the air and fuel specific impulse may be computed from the relations

$$I_a = \frac{T}{g\,\dot{m}_a} = \frac{u_e - u_0}{g} \tag{24}$$

and

$$I_f = \alpha I_a = \alpha_p\,(1+\mu)\,I_a \tag{25}$$

From the definition of the air specific impulse, the specific thrust follows as

$$\frac{T}{p_0\,A_{max}} = g\,\frac{\dot{m}_a}{p_0\,A_{max}}\,I_a \ .$$

Substituting $(1+\mu)\langle\dot{m}_j\rangle_{av}$ for $\dot{m}_a$ and then eliminating $\langle\dot{m}_j\rangle_{av}$ by means of Eq. (14), one obtains the specific thrust of the engine in the form

$$\frac{T}{p_0\,A_{max}} = (1+\mu)\,\frac{A_j}{A_{max}}\,\frac{I_a}{I_{aP}}\,\frac{T_P}{p_0\,A_j} \tag{26}$$

where the factor p_0 not only makes the equation nondimensional but also represents the effect of altitude on thrust.

B. Engines without mixing of the pulsejet exhaust with the shroud flow

If the shroud is made so short that no mixing of the pulsejet exhaust with the shroud flow takes place, the latter does not contribute directly to the thrust produced except for a drag due to losses in the duct. Except for these losses which will not be considered here, the shroud merely acts as a device that allows the pulsejet to operate with full utilization of ram precompression. Pulsejets operating under this condition were analyzed by Foa[2] and his method thus applies also to the case under consideration here.

In this method, combustion is approximated by a polytropic process but the value of the polytropic exponent depends greatly on the design of the pulsejet and cannot be determined theoretically at the present time. However, in Section IV.A the performance of the primary pulsejet at low flight Mach numbers had to be assumed and the value of the polytropic exponent was therefore determined from the condition that it would lead to a fuel specific impulse that is in agreement with the assumed value at a flight Mach number arbitrarily taken as 0.3. Although Foa's analysis includes an allowance for friction losses and also for variations of the specific heats, these effects are not taken into account here in order to keep the results comparable with those of the previous Section.

Unfortunately, this method does not allow the thrust of the engine to be determined and the work had to be limited to a calculation of the specific impulse values.

V. RESULTS OF THE ANALYSIS AND DISCUSSION

The results of the computations presented below are based on a performance of the primary pulsejet prescribed by

$$T_{Pn} / A_j = 360 \text{ lb/ft}^2$$

$$\alpha_p = 30$$

$$I_{fp} = 1200 \text{ and } 1800 \text{ sec.}$$

These values were selected as corresponding to an average pulsejet. The shroud design will be characterized by

$$A_j / A_{max} = 0.6$$

$$\mu = 2 .$$

Other constants used throughout the computations are:

$$h = 19{,}000 \text{ Btu/lb.}$$

$$\eta_c = 0.9$$

$$p_n = 2120 \text{ lb/ft}^2$$

$$\vartheta_n = 518 \ ^\circ\text{R}$$

$$\vartheta_o = 460 \ ^\circ\text{R}$$

$$R = 1718 \text{ ft.lb/slug } ^\circ\text{R}$$

$$c_p = 0.240 \text{ Btu/slug, } ^\circ\text{R}$$

$$\gamma = 1.40 .$$

Fig. 7 shows the fuel specific impulse plotted versus flight Mach number for completely ducted and tail ducted engines with and without mixing of the pulsejet exhaust with the surrounding flow; the fuel specific impulse of the primary engine is taken here as 1200 seconds and the parameter k which was introduced to allow for some uncertainty in the shroud flow is given the values 1.0 and 0.9, respectively. For comparison, the performance of a

ramjet computed according to the method of reference (2) is also included in the figures. It is based on the same over-all air/fuel ratio and the same assumptions for losses that are used for the ducted pulsejet. Fig. 8 gives the same plot but is based on a primary engine for which the fuel specific impulse is 1800 seconds. In Fig. 9, the specific thrust divided by the atmospheric pressure is plotted versus flight Mach number for the case I_{fp} = 1200 sec. This figure refers only to configurations with complete mixing. As pointed out before, the analysis in the case of no mixing allows only the specific impulse to be determined but not the thrust.

It is seen that the computed performance data are quite sensitive to comparatively small deviations of k from unity. It does not seem possible at the present time to obtain accurate values for k and for this reason, the presented values can only be considered as rough estimates of the potential performance of the ducted pulsejet. However, general trends may be noted and the following conclusions drawn from the results:

The augmentation effect due to mixing of the shroud flow with the pulsejet exhaust is very appreciable except in the range of lower flight Mach numbers. It is the more important the poorer the performance of the primary engine. At low flight Mach numbers, the primary pulsejet of an engine in which mixing takes place, acts as an intermittent ejector; instead of utilizing ram precompression, it operates at a pressure that is below ram pressure and may even be lower than atmospheric pressure. The advantage of the increased mass flow is then more than compensated by the mixing losses except for possible thrust augmentation at static operation or at extremely low flight velocities. The analysis, in the presented form, does not apply to this mode of operation and since the high-speed range was of particular

interest, it is the only one considered here. The above conclusions are in agreement with similar ones reached by Sänger[4].

For subsonic flight Mach numbers, the analysis leads to the same results for a completely ducted and a tail ducted engine because any difference would be due to a difference of friction losses in the two configuration that have not been considered. In this range of flight velocities, the tail ducted engine would therefore be more promising because the losses in the narrow passage between the pulsejet combustion chamber and the shroud (see Fig.1) of a completely ducted engine would be avoided. Furthermore, a tail ducted engine might be constructed with a smaller frontal area than a completely ducted engine for the same ratio A_j / A_{max} .

Shock losses of a completely ducted engine are lower than those of a tail ducted one. This may offset the initial advantage of the latter configuration and may make the completely ducted pulsejet the superior engine in the range of supersonic flight velocities.

At high Mach numbers, the performance of a ducted pulsejet in which mixing takes place is not much different from that of a ramjet operating at the same over-all air/fuel ratio. However, for decreasing flight Mach numbers, the performance of the ramjet falls off faster than that of the ducted pulsejet. This shows that at high flight Mach numbers, the ducted pulsejet is simply a ramjet in which the "flame holder" contributes a small thrust (or even a drag) while at low flight Mach numbers the characteristics of the conventional pulsejet become more apparent.

The specific thrust of the ducted pulsejet operating with complete mixing of its exhaust with the shroud flow may reach fairly high values although not as high as those that could be obtained with a ramjet operating

at an air/fuel ratio closer to stoichiometric, or with a turbojet. The main advantage of the ducted pulsejet would seem to lie in its capability of producing useful thrust at low flight velocities when compared to the ramjet, and in its simplicity when compared to the turbojet.

It was pointed out before that in the case of engines in which no mixing takes place, ducting merely represents a scheme to obtain pulsejet operation with full utilization of ram precompression. An unducted engine working under the same conditions would have the advantage of considerably smaller size for the same performance but no method to achieve this has been successfully demonstrated so far.

The computed performance data refer to engines that are designed for the Mach number under consideration. The selected values for the design parameters (e.g., the mass flow ratio) apply only at the design Mach number and assume different values at other Mach numbers. The curves thus represent the potential performance at any Mach number and not the performance of an engine of fixed configuration. It appears desirable, however, to have the shroud adjustable in flight to permit utilization of mixing only in the range of Mach numbers in which it is advantageous.

No test data for ducted pulsejets are available that could be compared with the presented results. Such tests would not only have to yield information about thrust and fuel consumption but would also have to supply details of the internal flow conditions since without the latter, any comparison between theory and experiments would be meaningless.

Although it has not been possible to make accurate predictions regarding the potential performance of the ducted pulsejet, the results indicate that this engine type could find use in applications involving high subsonic and low supersonic flight velocities.

VI APPENDIX

Some Experimental Studies of the Flow Inside the Shroud near the Tail Pipe Exit of the Pulsejet

Two different experiments that had been performed in the early phases of this program effectively supported the conclusion reached in Section III.B, namely, that the flow around the tail pipe is practically brought to rest periodically by the intermittent exhaust from the pulsejet.

The first experiment was based on the analogy between surface gravity waves in shallow water and pressure waves in ducts[6]. The model of a tail ducted pulsejet was set into a tank of shallow water the depth of which was approximately 0.5 inch. Periodic waves leaving the tail pipe were produced by an electrically driven pendulum that was submerged in the "combustion chamber". The flow was visualized by small droplets of ink on the water surface. At the correct frequency of the pendulum an intermittent jet was formed[9] which induced flow through the shroud by drawing particles from the shroud into the tail pipe and then ejecting them downstream. It could be clearly observed that the particles on the outside of the tail pipe moved intermittently with definite stops in their motion.

In a second experiment, the tail pipe of a small pulsejet was surrounded by a transparent duct. The exhaust again induced a pulsating flow that was visualized by strongly illuminated smoke particles. High speed motion pictures taken at about one thousand frames per second also demonstrated the inflow into the tail pipe and the intermittent motion of the particles on the outside of the tail pipe, particularly of those that were close to the pulsejet walls.

VII ACKNOWLEDGMENTS

The author wishes to thank Dr. J. V. Foa for valuable discussions during the course of the work, and to Miss A. Adams and Mrs. M. Beale Johnson who handled the large amount of computing that was required. The mentioned experiments with small pulsejet models were carried out by Mr. J. Logan, Jr.

REFERENCES

1. L.B.Edelman, The pulsating jet engine – its evolution and future prospects, SAE Quarterly Transactions 1, 204–216, 1947.
2. J.V.Foa, Single flow jet engines – a generalized treatment, Journal of the American Rocket Society,21,115–126 and 131, Sept.1951.
3. G. Rudinger, An evaluation of the potential merits of ducted pulsejets, Project SQUID, Technical Memorandum No. CAL–32, October 1949.
4. E. Sänger, Luftzumischung zu Abgasstrahlen, Ingenieur-Archiv, 18, 310–323, 1950.
5. J.V.Foa, Mach number functions for ideal diatomic gases, Cornell Aeronautical Laboratory, Inc., October 1949.
6. e.g., R. Courant and K.O. Friedrichs, Supersonic flow and shock waves, Interscience Publishers, Inc., New York, 1948.
7. J.H.Hett & R.W.King, Jr., A frequency modulation pressure recording system. Review of Scientific Instruments, 21, 150–153, February 1950.
8. A. Kantrowitz and C. Donaldson, Preliminary investigation of supersonic diffusers, NACA Wartime Report, originally issued as ACR No. L5D20, May 1945.
9. G. Rudinger, J. Logan, Jr., and O.B.Finamore, Investigation of Acoustic Jets, Part Two, Project SQUID, Technical Memorandum No. CAL–18, 20 April 1948.

CONFIGURATION OF A DUCTED PULSEJET

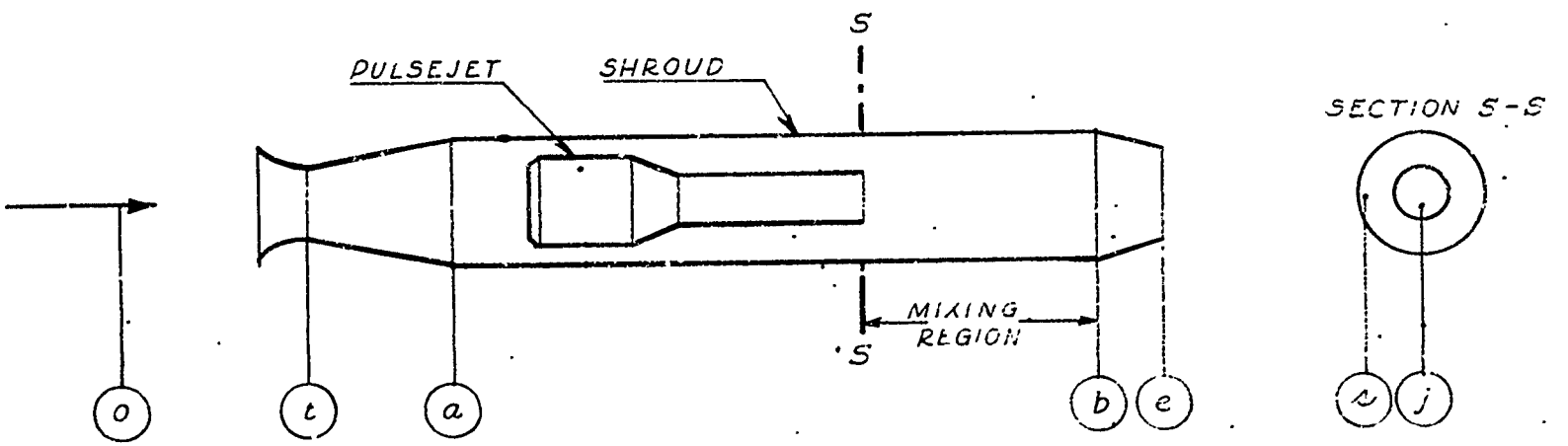

Fig. 1

SHOCK WAVES ORIGINATING
AT THE PULSEJET VALVES

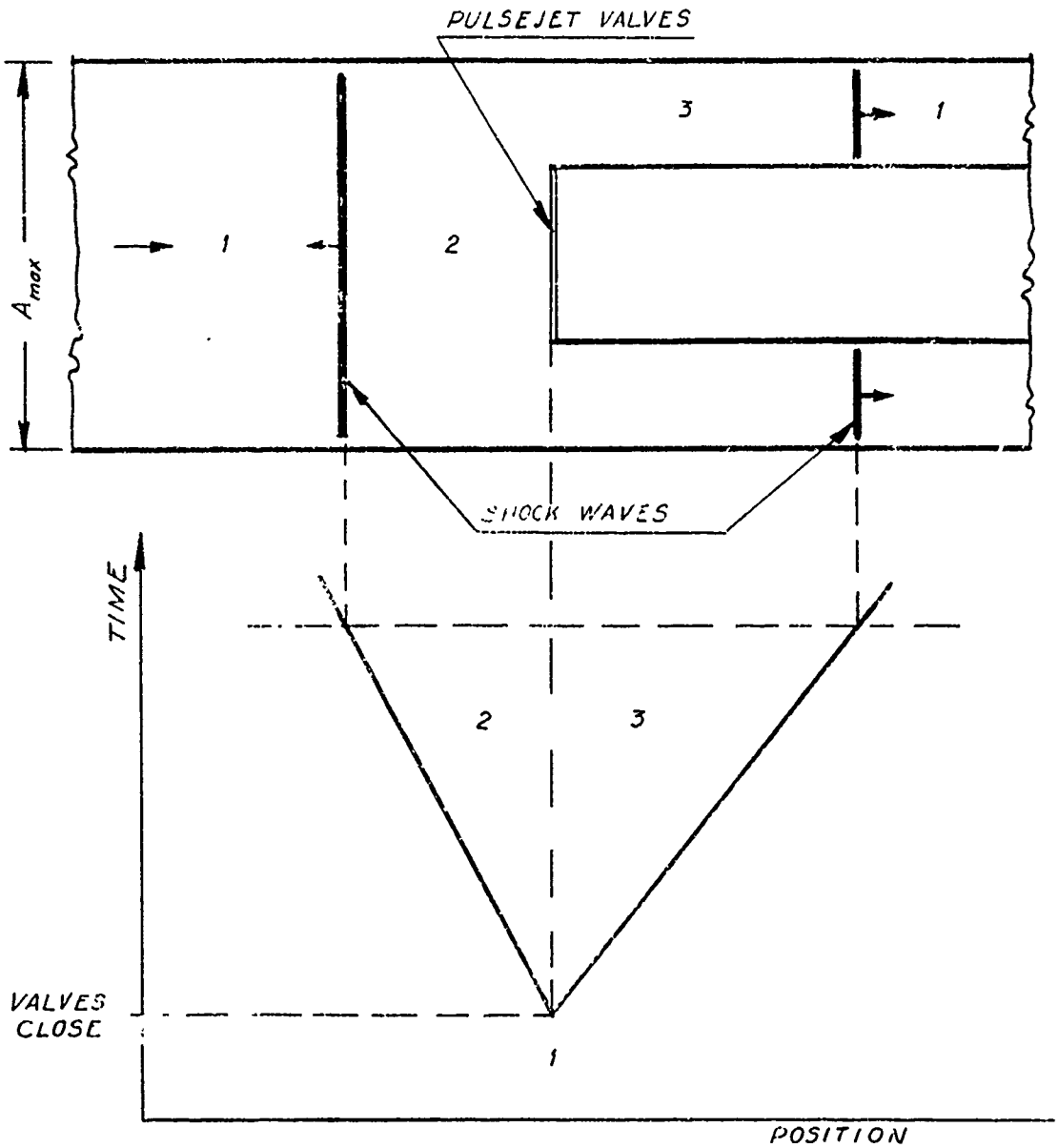

Fig 2

STRENGTH OF THE SHOCK WAVES ORIGINATING AT THE PULSEJET VALVES

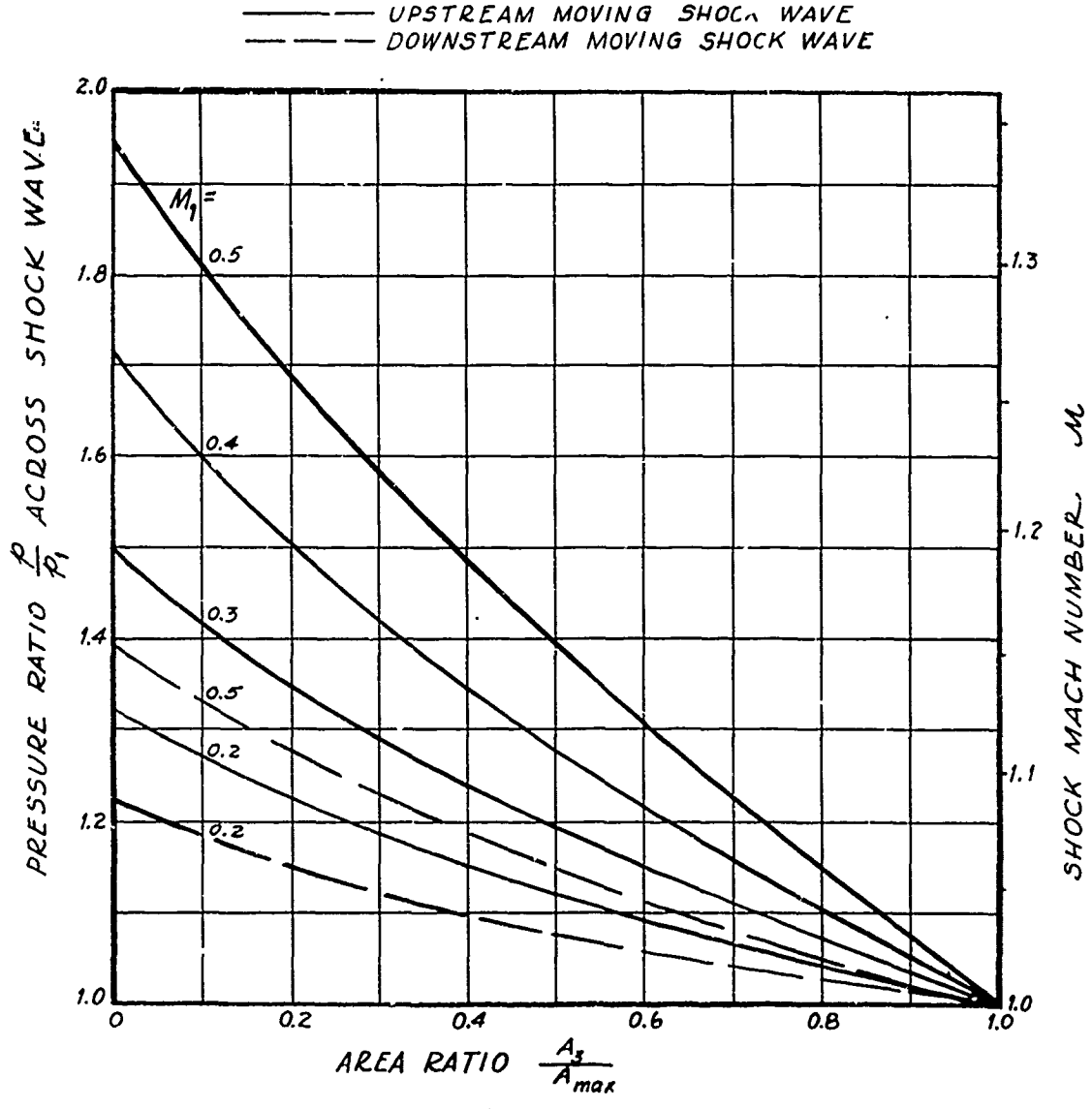

Fig. 3

SHOCK WAVES ORIGINATING AT THE PULSEJET EXIT

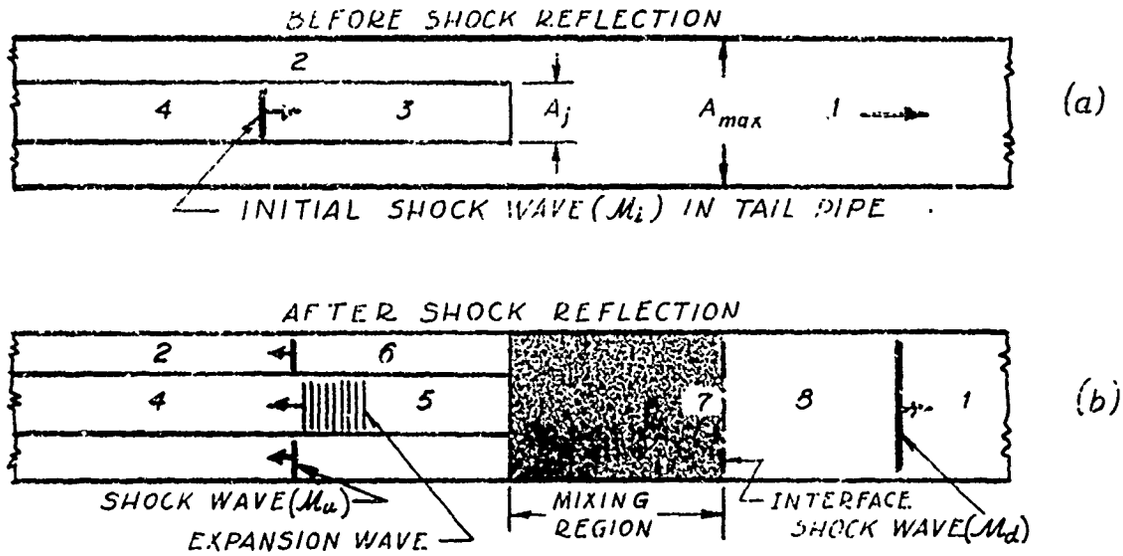

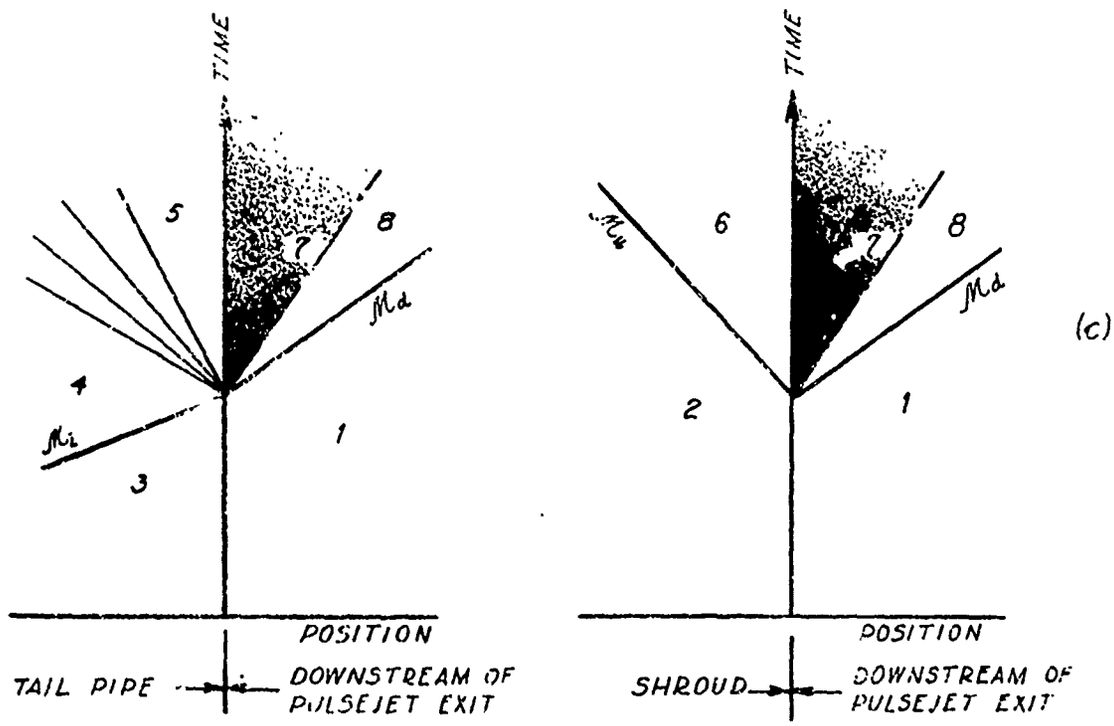

Fig. 4

STRENGTH OF UPSTREAM MOVING SHOCK WAVES
ORIGINATING AT THE PULSEJET EXIT

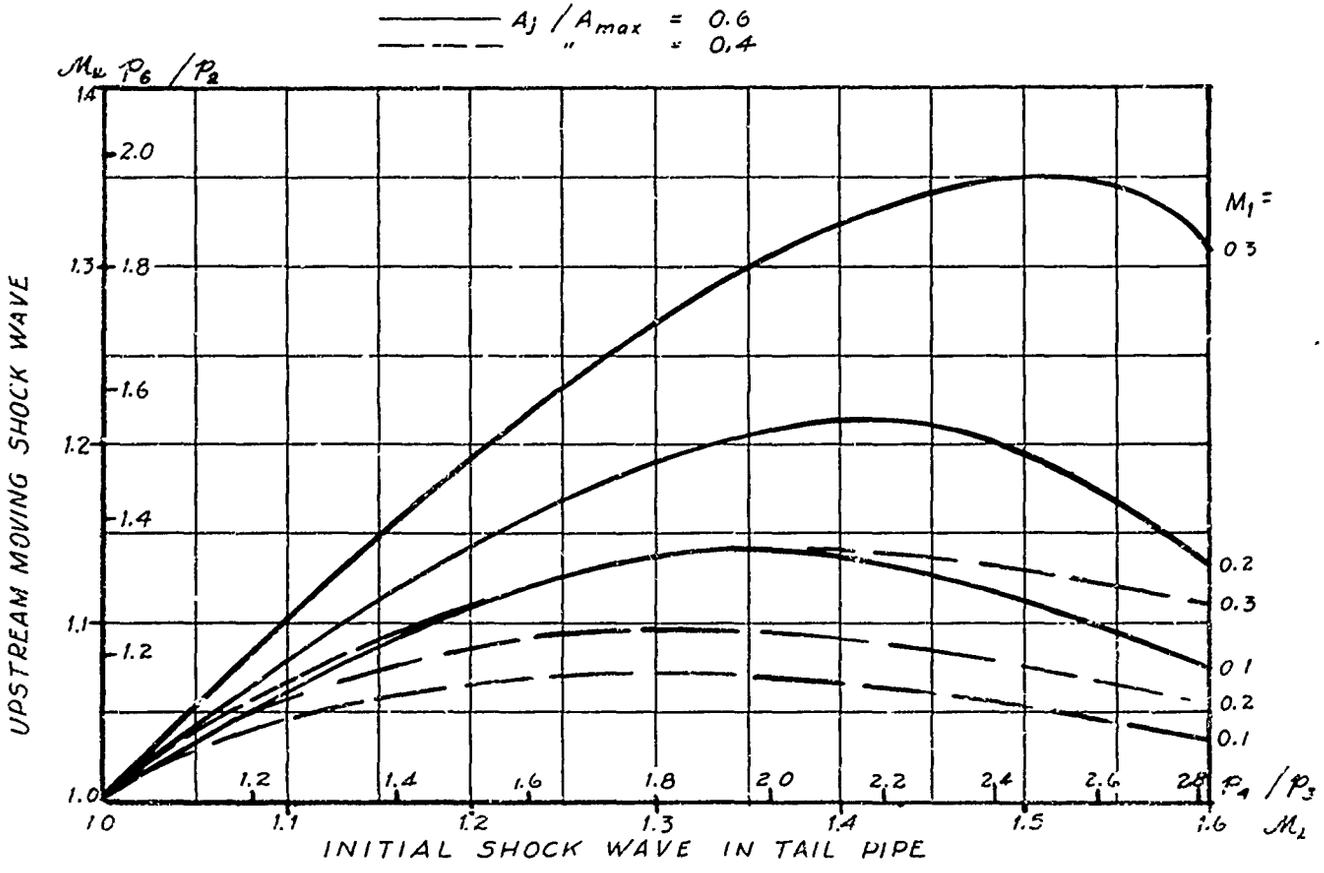

Fig. 5

STRENGTH OF DOWNSTREAM MOVING SHOCK WAVES
ORIGINATING AT THE PULSEJET EXIT

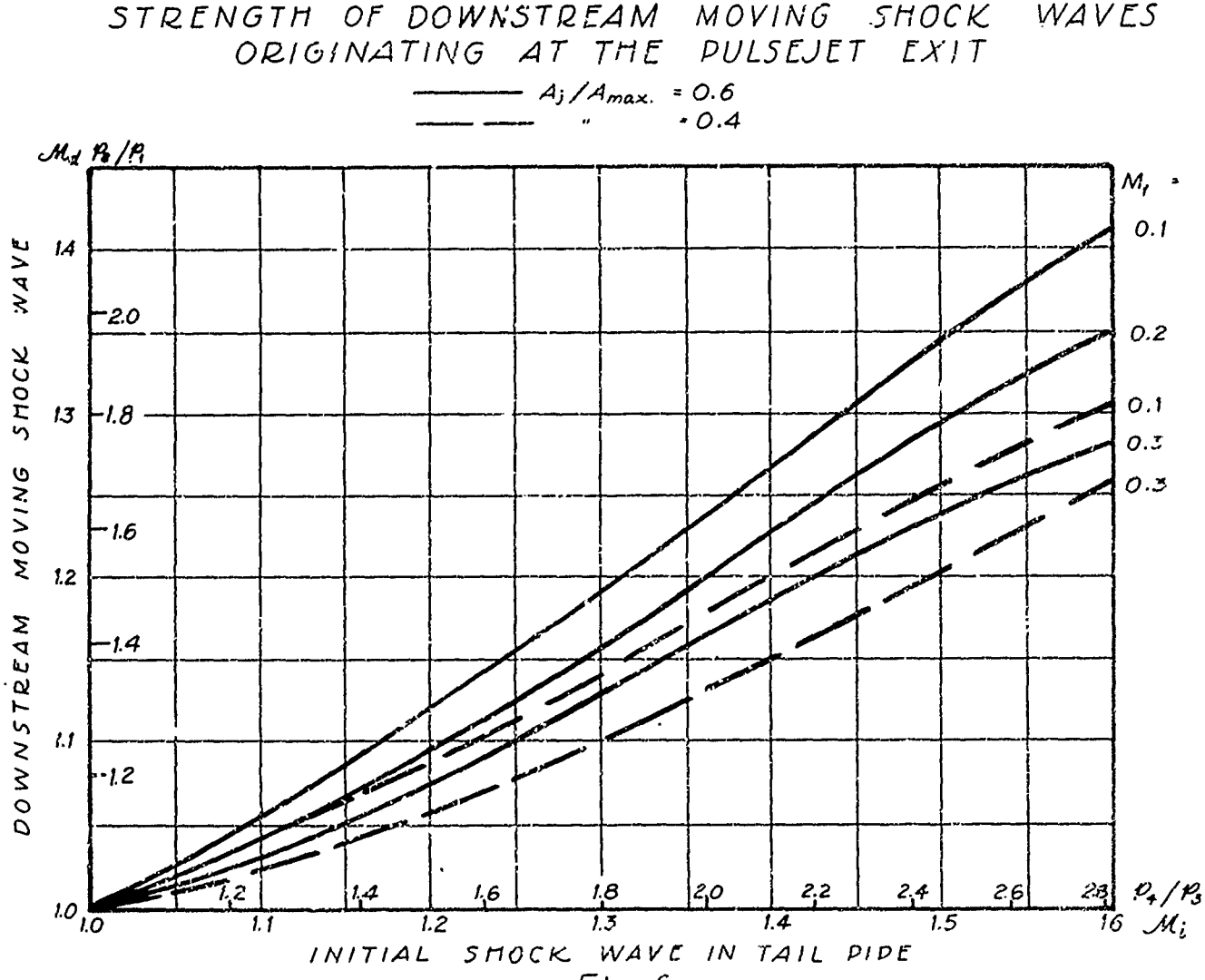

Fig. 6

FUEL SPECIFIC IMPULSE OF THE DUCTED PULSEJET

$A_j / A_{max} = 0.6$
$\mu = 2$
$\alpha_p = 30$
$I_{fp} = 1200$ SEC.
$T_{Pn} / A_j = 360$ LB/FT^2

—— COMPLETELY DUCTED ENGINE
– – – TAIL DUCTED ENGINE

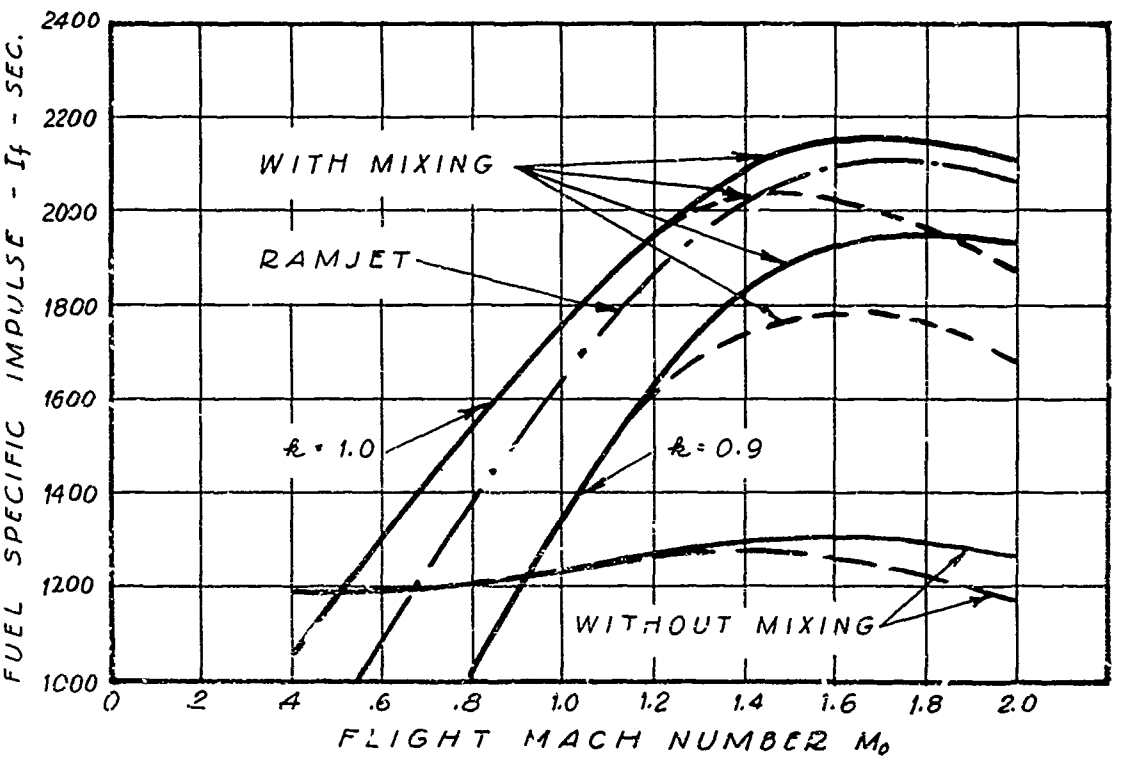

FRICTION LOSSES WHICH ARE HIGHER FOR COMPLETELY DUCTED THAN FOR TAIL DUCTED ENGINES ARE NOT CONSIDERED.

Fig. 7

FUEL SPECIFIC IMPULSE OF THE DUCTED PULSEJET

A_j / A_{max} = 0.6
μ = 2
α_p = 30
I_{fp} = 1800 SEC.
T_{Pn} / A_j = 360 LB/FT²

—— COMPLETELY DUCTED ENGINE
--- TAIL DUCTED ENGINE

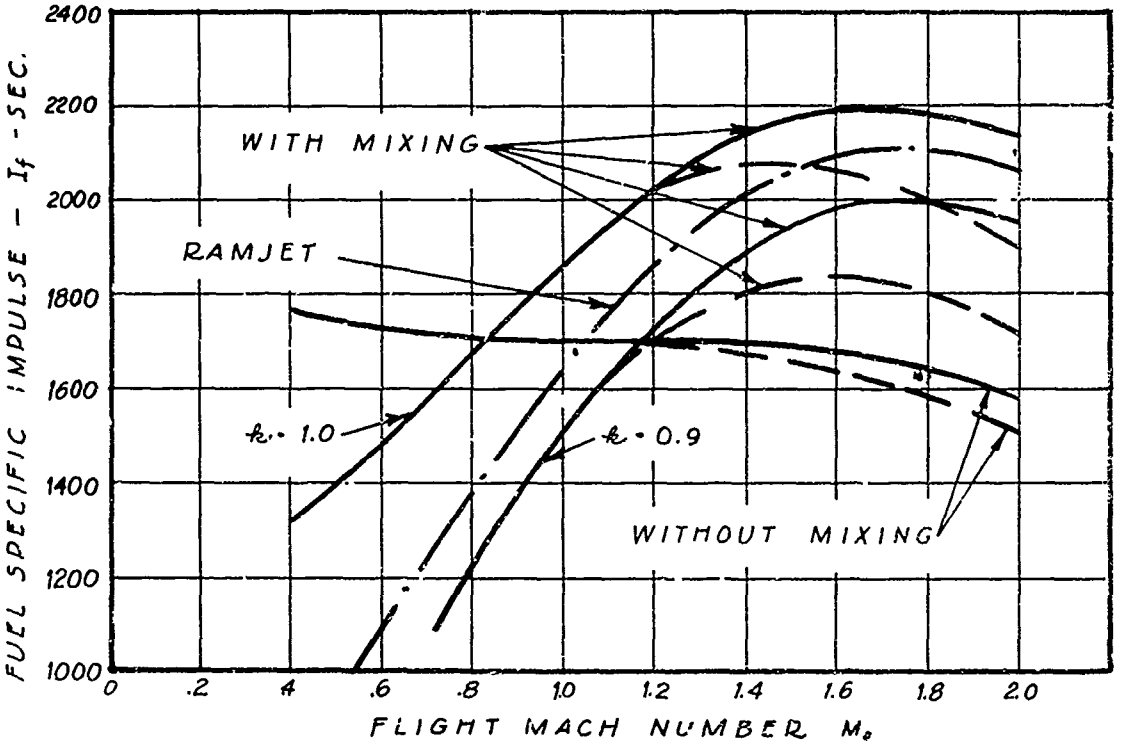

FRICTION LOSSES WHICH ARE HIGHER FOR COMPLETELY DUCTED THAN FOR TAIL DUCTED ENGINES ARE NOT CONSIDERED.

Fig. 8

SPECIFIC THRUST OF THE DUCTED PULSEJET
(WITH COMPLETE MIXING)

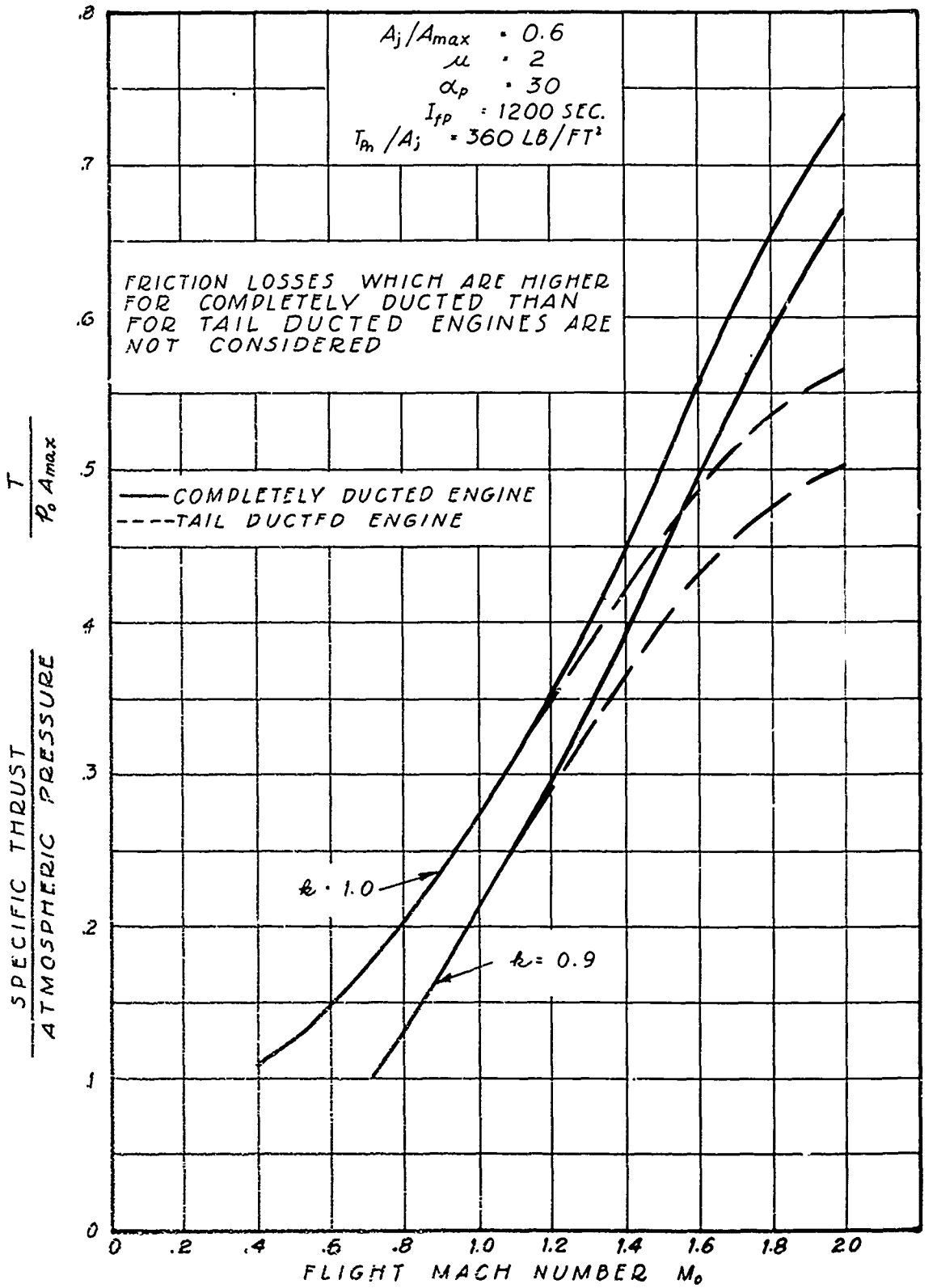

Fig. 9

DISTRIBUTION LIST

PARTS A,B,C, and DP of the A.N.A.F.G.M. Mailing List, July 1951

1. H.S.Taylor, Princeton University
2. J.V.Charyk, Princeton University
3. F. Clauser, Johns Hopkins University
4. J.V.Foa, Cornell Aeronautical Laboratory
5. N.J.Hoff, Polytechnic Institute of Brooklyn
6. M.J.Zucrow, Purdue University
7. K. Wohl, University of Delaware
8. G.Markstein, Cornell Aeronautical Laboratory
9. R.N.Pease, Princeton University
10. P.Libby, Polytechnic Institute of Brooklyn
11. S.A.Guerrieri, University of Delaware
12. L. Lees, Princeton University
13. G.Rudinger, Cornell Aeronautical Laboratory
14. S.W.Yuan, Polytechnic Institute of Brooklyn
15. P.K.Porter, Cornell Aeronautical Laboratory
16. H.J.Shafer, Princeton University
17. A.P.Colburn, University of Delaware
18. G.S.Meikle, Purdue University
19. J.J.O'Neil, Cornell Aeronautical Laboratory
20. R.J.Woodrow, Princeton University
21. F.A.Parker, Princeton University
22. M.Summerfield, Princeton University
23. W.J.Barr, Princeton University
24. J.H.Waxelin, Textile Research Foundation
25/37. Chief of Naval Research, Code 429, Washington, D.C.(13cc)
38. Commanding Officer, O.N.R., New York, New York
39. Commanding Officer, O.N.R., Chicago, Illinois
40. Commanding Officer, O.N.R., Boston, Mass.
41. Commanding Officer, O.N.R., San Francisco, Calif.
42. Commanding Officer, O.N.R., Pasadena, Calif.
43/45. Chief, Bureau of Aeronautics, Power Plant Div., Exp.Engines Branch (3)
46. Chief, Bureau of Aeronautics, Power Plant Div., Fuels and Lubricants Branch
47. Chief, Bureau of Aeronautics, Ship Installations Div.
48. P.Kratz, O.N.R. Reg.Representative, Philadelphia, Penna.
49. Commander R.W.Pickard, Buaer Representative, Cornell Aeronautical Laboratory, Buffalo, New York
50. D.G.Samaras, Office of Air Research, Wright-Patterson Air Force Base
51/52. F.Tanczos, Bureau of Ordnance, Guided Missiles Division, Washington, (2)
53. W.Worth, Power Plant Laboratory, Engineering Div., Wright Field
54. C.F.Yost, Directorate of Research and Development, USAF, Pentagon
55/56. Chief of Naval Research, Navy Research Section, Library of Congress(2)
57. W.Tenney, Aeromarine Company
58. R.Folsom, University of California, Mechanical Engineering Department
59. Engineering Librarian, Columbia University Library
60. C.Millikan, Guggenheim Aeronautical Laboratory, California Institute of Tech.
61. B.L.Crawford, Department of Chemistry, University of Minnesota
62. Officer in Charge, Naval Ordnance Test Station, Pasadena, Calif.
63. J. Moriarty, Purdue University Library
64. B. Lewis, Bureau of Mines, Pittsburgh, Penna.
65. L.Crocco, Princeton University
66. Manson Benedict, Hydrocarbon Research, Inc., New York City

67. Gerhard Dieke, Johns Hopkins University
68. M.W.Evans, 3115 Western Avenue, Park Forest, Chicago Heights, Illinois
69. K.F.Hertzfeld, Department of Physics, Catholic University of America
70. Arnold Kuethe, University of Michigan, Ann Arbor, Michigan
71. C.C.Lin, Dept. of Aero. Eng., Massachusetts Institute of Technology
72. A.J.Narad, Consulting Engineering Lab., General Electric, Schenectady
73. W.R.Sears, Graduate School of Aeronautical Engineering, Cornell University
74. Guenther von Elbe, U.S.Bureau of Mines, Central Exp. Station, Pittsburgh
75. G. Henning, Aerojet Engineering Corp., Azusa, California
76. J.B.Henry, Allegheny Ludlum Steel Corp., Breckenridge, Penna.
77. L.N.K. Boelter, University of California, Los Angeles, Calif.
78. Committee on Undersea Warfare, National Research Council, Wash.
79. P.A.Lagerstrom, Guggenheim Aero.Lab., California Institute of Technology
80. J.Keenan, Massachusetts Institute of Technology, Cambridge, Mass.
81. J.D.Akerman, University of Minnesota, Minneapolis, Minn.
82. W.A.Wildhack, National Bureau of Standards, Washington, D.C.
83. Buffalo-Electro Chemical Corporation, Buffalo, New York
84. R. Ladenburg, Princeton University, Physics Department
85. D.H.Hill Library, University of North Carolina, Raleigh, North Carolina
86. I.T.E.-Circuit Breaker Company, Special Products Div., Philadelphia, Pa.
87. Aircooled Motors, Inc., Syracuse, New York
88. AiResearch Manufacturing Company, Los Angeles, Calif.
89. Allison Division, General Motors Corporation, Indianapolis, Indiana
90. B.G.Corporation, New York
91. Champion Spark Plug Company, Toledo, Ohio
92. Fredric Flader, Inc., North Tonawanda, New York
93. General Electric Company, Aircraft Gas Turbines Div., West Lynn, Mass.
94. General Laboratory Associates, Inc., Norwich, New York
95. Lycoming-Spencer Div., Avco Manufacturing Corporation, Williamsport, Pa.
96. McCulloch Motors Corporation, Los Angeles, California
97. Pratt and Whitney Aircraft Division, U.A.C., East Hartford, Conn.
98. Stalker Development Company, Bay City, Michigan
99. Stanford University, Stanford, Calif.
100. Thompson Products Inc., Cleveland, Ohio
101. University of Southern California, Los Angeles, Calif.
102. Westinghouse Electric Corporation, A.G.T. Division, Essington, Pa.
103. Kenneth Razak, Acting Dean, College of Business Administration and Industry, University of Wichita, Wichita, Kansas
104/106. Cornell Aeronautical Library, 4455 Genesee Street, Buffalo, N.Y. (3)
107. Georgia Institute of Tech., Dept.of Mechanical Eng., Atlanta, G. Attn: Prof. M.J.Goglia
108. Dr. R.B.Dow, BuOrd, Navy Dept. (Re9a)
109. Dr. R.M.Robertson, O.N.R., Washington, D.C.
110. Dr. Ralph Zirkind, BuAer, Navy Department, Washington, D.C.
111. Lt.Col.J.H.Clayton, AFDRD-RE-1, A/F, Director Research and Development Pentagon, Washington, D.C.
112. Dr. A.M.Rothrock, N.A.C.A.
113. Atlantic Research, 812 N. Fairfax Street, Alexandria, Va.
114. Chief, Bureau of Aero.Ships Installation Div.Rocket Branch, Navy Dept. Washington, D.C.
115. Dr. R.H.Wilhelm, Chemical Eng. Building, Princeton University
116. Mr. J.P.Layton, Princeton University
117. Dr. Mark M. Mills, Princeton University

118. Mr. J.A.Browning, Dartmouth University, Hanover, N.H.
119. Professor G.C.Lamb, Northwestern University, Evantons, Illinois
120. Dr. A. Ferri, N.A.C.A. Langley Field, Virginia
121. Professor W.M.Rohsenow, M.I.T., Cambridge, Mass.
122. Mr. H. Hottel, M.I.T. Cambridge, Mass.
123. Professor F.G.Keyes, M.I.T. Cambridge, Mass.
124. Professor E. Johnson, Princeton University